Interparticle Coulombic Decay Dynamics along Single- and Double-Ionization Pathways

Fabian Langkabel,[†,‡] Martin Lützner,[†,¶,§] and Annika Bande[*,†]

†*Helmholtz-Zentrum Berlin für Materialien und Energie GmbH, Albert-Einstein-Str. 15, 12489 Berlin, Germany*

‡*Department of Chemistry, Humboldt-Universität zu Berlin, Brook-Taylor-Str. 2, 12489 Berlin, Germany*

¶*Department of Physics, Freie Universität Berlin, Arnimallee 14, 14195 Berlin, Germany*

§*Institute of Chemistry und Biochemistry, Freie Universität Berlin, Takustr. 3, 14195 Berlin, Germany*

E-mail: annika.bande@helmholtz-berlin.de

Abstract

The interparticle Coulombic decay process (ICD) in a Coulomb-coupled pair of quantum dots (QDs) was predicted to feature electronic relaxation within one QD in conjunction with ionization of the other. In this work the QD model is extended from a pair to a triad of one excited and two ionizable QDs and in total three electrons. Analytical Wigner-Weisskopf expressions for the decay rates are formulated and confirmed with numerical electron dynamics calculations, suggesting a rate enhancement by a factor two that may be relevant for the competitiveness of ICD in QDs. Particularly, we compare two energetic scenarios, one allowing only for single ionization of the QD triad and one, not yet discussed in the community, potentially allowing for double ionization.

Introduction

Energy transfer possibly coupled to energy conversion is an emerging concept grace to its manifold of occurrences ranging from a chain of Förster resonant energy transfer steps in biological processes[1] to solar energy devices.[2] In recent years, the interparticle Coulombic decay (ICD) process has gained much attention because it goes beyond resonance energy transfer among bound-to-bound electronic transitions by including one bound-to-continuum transition and being at the same time about three orders of magnitude faster, while exhibiting otherwise the same characteristics of being mediated by long-range Coulomb interaction alone. This was first demonstrated in clusters of HF and of H_2O molecules, where the inner-valence excitation of one monomer decays upon ionization of a neighbor.[3] Over the years ICD turned out to be a very general process, hence it appears in very different fields[4] and cutting edge examples are photo damage of biological tissue,[5,6] relaxation of hollow atoms,[7] vibrational energy transfer,[8] and effectiveness in fullerenes.[9,10]

The concept of ICD of converting optical into electric energy together with its anticipated relevance to nanomaterials makes it promising for optoelectronic devices. And indeed it has been predicted for pairs of non-tunneling coupled semiconductor quantum films[11] as well as quantum dots.[12,13] The only drawback is that, compared to clusters of atoms and molecules of smaller spatial dimensions, ICD was found to be significantly slower happening on a picoseconds rather than a femtosecond time scale. On such time scale phonon dissipation might become competitive.[14] Opposed to this there is evidence for an ICD rate enhancement with the number of reaction channels, i.e. neighbors.[7,15,16] Therefore we seek to speed ICD along these lines and will offer for this the first predictions for ICD in a triad of QDs which is at the same time the first electron dynamics calculation of ICD with three participating electrons.

In extension to what is typically done in atomic and molecular clusters, we will probe different energetic boundary conditions by examination of different QD geometries. This aligns well with the fact that QDs are probably the quantum material with the largest

wealth of electronic structures tuneable as desired by size, shape, and surface of the QD.[17,18] We modify the electronic structure in this way to elaborate on the possibility of a double-ionization ICD process. A first energetic argument for it was given for endohedral fullerens,[9] however, without estimation on its rate. It was observed recently in Helium droplets with neighboring alkali dimers,[19] but there without detailed theoretical analysis.

To transport the two messages on rate enhancement and double-ionization ICD in this article we will start from the known QD pair system, extend the expression for the ICD rate from the case of one neighbor to the case for two neighbors, and confirm both of them numerically with electron-dynamics calculations. This we do in comparison for two sets of QD triads, one excluding and one allowing for double-ionization ICD.

Theory

Two-Electron Two-QD ICD

For the QD pair let's assume first of all QDs well separated from each other, which means they shall neither form delocalized orbitals nor allow for electron tunneling as would be the case in a QD molecule.[20] Further, the QDs shall be singly charged and display one and two electronic levels below the single-electron ionization threshold energy $E_T = 0$ meV that obey the energy condition $E_{M1} - E_{M0} \leq E_T - E_{R0}$ (cf. Fig. 1, middle and right QD, MQD and RQD). Excitation of the electron in the two-level MQD will create a localized two-electron resonance state M_1R_0 (dashed-line density above QDs, however with zero density above the displayed left QD (LQD)) that decays into the multitude of continuum states M_0C. The originally excited electron occupies again its ground state, whereas the RQD is ionized. In electron dynamics calculations on GaAs QDs the rate Γ^{2e} for this two-electron ICD process was found earlier,[13,21] and here again, to be among $4.13 \cdot 10^{-3}$ - $2.85 \cdot 10^{-9}$ meV ($1.59 \cdot 10^{2}$ - $2.31 \cdot 10^{8}$ ps) and to sensitively depend on the distance R among the QDs, which was $87-867$ nm.

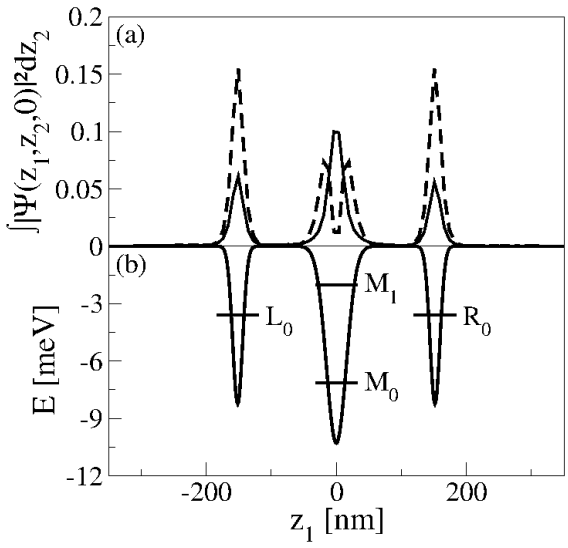

Figure 1: In the bottom (b) the model potential for the QD triad as function of one of the z coordinates and the contained single-electron energy levels are displayed. On top (a) the density of the wave packets of the resonance (dashed line) and ground state (solid line) are shown. For the two-electron two-QD case the LQD with above density is omitted and the z coordinate origin shifted to $R/2$.

Starting from the general golden rule of Fermi,

$$\Gamma^{2e} \propto |\langle f|V_C^{12}|d\rangle|^2, \tag{1}$$

an explicit expression for the ICD rate in the above two-electron two-QD case,

$$\Gamma^{2e} = |\langle \phi_1^{M0}\phi_2^C|V_C^{12}|\phi_1^{M1}\phi_2^{R0}\rangle|^2, \tag{2}$$

was developed in a Wigner-Weisskopf framework.[15,22] In Eq. (2), the Coulomb interaction operator $V_{12}^C = |\vec{r_1} - \vec{r_2}|^{-1}$ couples the decaying state $|d\rangle = \left|\phi_1^{M1}\phi_2^{R0}\right\rangle$ with the multitude of final states $|f\rangle = \left|\phi_1^{M0}\phi_2^C\right\rangle$. Note that for all wave functions we assume separability into a product of single-electron orbital functions. When we further do not take antisymmetry into account, which is possible as exchange terms were found to become negligible for the requested long distance among the adjacent QDs whose orbitals ϕ^n are not overlapping,[13,15] then we may deliberately assign electron no. 1 to be located in the MQD occupying the

M_1 or M_0 state and electron no. 2 being ionized from the initial R_0 state of the RQD into the continuum states (C). The process nails then down to the two Coulomb-coupled dipole transitions of the same energy difference on the subsystems M and R. With replacing all remaining direct Coulomb terms by dipole-dipole coupling terms one ends up with the known and proven analytical and asymptotic equation[22]

$$\Gamma^{2e} = \frac{3c^2\hbar^4}{4\pi} \frac{\sigma_R^{PI}(E_{vph})\Gamma_M^{rad}}{E_{vph}^4 R^6} \tag{3}$$

which approximates the long-distance behavior of the ICD rate. Here, E_{vph} stands for the energy of the transferred so-called virtual photon, $\sigma_R^{PI}(E_{vph})$ for the photoionization cross section of the electron-emitting RQD as function of that energy,[23] and Γ_M^{rad} for the radiative decay rate of the photon-emitting MQD.

The described approach already dates back about half a century, when it was introduced with a full derivation first for the Penning ionization[24] and then for the Auger process.[25] Later it was adapted to ICD and termed virtual photon approximation.[15,22]

In the context of atomic and molecular ICD, the rate ansatz of Eq. (2) as well as the asymptotic equation of Eq. (3) have been generalized for cases in which the decaying subsystem has $N > 1$ identical neighbors capable of electron emission.[15] It predicts a rate

$$\Gamma^{(N+1)e} = N \cdot \Gamma^{2e} \tag{4}$$

for $(N+1)$ subsystems with $(N+1)$ electrons involved in ICD that linearly depends on the number of neighbors N.[15,22]

A numerical proof of Eq. (4) using non-Hermitian electronic structure methods was given in a system of a Ne atom in a neighborhood of $N = 1-4$ other Ne atoms at equal distance, one of which can be ionized.[15,16] However, for $N = 4-12$ the predicted linearity was lifted for the sake of significantly higher rates, which the authors rationalized by increasingly important neighbor-neighbor correlation effects. The effect of such an extraordinary rate

increase was recently also seen in the deexcitation of hollow noble gas atoms in an ICD with numerous adjacent carbon atoms of a nearby graphene surface.[7]

Three-Electron Three-QD ICD

Here, we assume three well-separated singly-charged QDs, a QD triad, in a nanowire structure with the photo-emitting dot in the central place (MQD in Fig. 1). The electronic structure design in QDs allows it to realize two different energy regimes. One is allowing for ionization of only one QD at a time (as in Ne) and the other for ionizing both simultaneously. This aspect to ICD has not found much consideration yet, as it is typically not relevant in molecular systems.

The Wigner-Weisskopf ansatz is independent of the regime. The Coulomb operator $V_C = V_C^{12} + V_C^{23} + V_C^{13}$ sums over the three pairwise interaction terms. Under the same assumptions of orbital product wave functions and a spin-free formulation for electrons on distant QDs, the decaying state's wave function is $|d\rangle = |\phi_1^{L0}\phi_2^{M1}\phi_3^{R0}\rangle$ with assigning electron numbers to QDs as $1 \Leftrightarrow$ LQD, $2 \Leftrightarrow$ MQD, and $3 \Leftrightarrow$ RQD. Electrons with indices 1 and 3 are equivalent throughout.

Only the final state wave function depends on the energetics of the system. If $2 \cdot IP > \Delta E_M > 1 \cdot IP$, where IP signifies ionization potential, then either the left or the right QD can be ionized and the final state is a superposition of electron 1 or 3 in the continuum, i.e. $|f\rangle = 2^{-1/2}\left(\left|\phi_1^{L0}\phi_2^{M0}\phi_3^{C}\right\rangle + \left|\phi_1^{C}\phi_2^{M0}\phi_3^{R0}\right\rangle\right)$. Writing out the Wigner-Weisskopf ansatz for the single-ionization (SI) case and separating the integrals gives

$$
\begin{aligned}
\Gamma_{SI}^{3e} \;\propto\; & |2^{-1/2}(\langle\phi_1^{L0}\phi_2^{M0}|V_C^{12}|\phi_1^{L0}\phi_2^{M1}\rangle\langle\phi_3^{C}|\phi_3^{R0}\rangle \\
+ \; & \langle\phi_2^{M0}\phi_3^{C}|V_C^{23}|\phi_2^{M1}\phi_3^{R0}\rangle\langle\phi_1^{L0}|\phi_1^{L0}\rangle \\
+ \; & \langle\phi_1^{L0}\phi_3^{C}|V_C^{13}|\phi_1^{L0}\phi_3^{R0}\rangle\langle\phi_2^{M0}|\phi_2^{M1}\rangle) \\
+ \; & 2^{-1/2}(\langle\phi_1^{C}\phi_2^{M0}|V_C^{12}|\phi_1^{L0}\phi_2^{M1}\rangle\langle\phi_3^{R0}|\phi_3^{R0}\rangle \\
+ \; & \langle\phi_2^{M0}\phi_3^{R0}|V_C^{23}|\phi_2^{M1}\phi_3^{R0}\rangle\langle\phi_1^{C}|\phi_1^{L0}\rangle
\end{aligned}
$$

$$+ \quad \langle\phi_1^C\phi_3^{R0}|V_C^{13}|\phi_1^{L0}\phi_3^{R0}\rangle\langle\phi_2^{M0}|\phi_2^{M1}\rangle)|^2. \tag{5}$$

We can rationalize that for orthonormal single-electron functions (that are identical for all identical electrons) only the second and fourth row of Eq. (5) give a non-zero contribution. Hence, $\Gamma_{SI}^{3e} = 2 \cdot \Gamma^{2e}$ in accordance with previous findings.[15]

By contrast, in the double-ionization (DI) ICD regime the virtual photon energy exceeds twice the ionization potential, i.e. $\Delta E_M > 2 \cdot IP$, so it allows for the final states $|f\rangle = \left|\phi_1^C\phi_2^{M0}\phi_3^C\right\rangle$. The respective equation for the ICD rate gives

$$\begin{aligned}\Gamma_{DI}^{3e} \quad &\propto \quad |\langle\phi_1^C\phi_2^{M0}|V_C^{12}|\phi_1^{L0}\phi_2^{M1}\rangle\langle\phi_3^C|\phi_3^{R0}\rangle \\ &+ \quad \langle\phi_2^{M0}\phi_3^C|V_C^{23}|\phi_2^{M1}\phi_3^{R0}\rangle\langle\phi_1^C|\phi_1^{L0}\rangle \\ &+ \quad \langle\phi_1^C\phi_3^C|V_C^{13}|\phi_1^{L0}\phi_3^{R0}\rangle\langle\phi_2^{M0}|\phi_2^{M1}\rangle|^2. \end{aligned} \tag{6}$$

All factorized integrals become zero due to the orthonormality of the single-particle functions so that $\Gamma_{DI}^{3e} = 0$. The result reveals that opening the DI channel does not mean ICD is capable of ionizing two QDs simultaneously during energy transfer. This is logical, because the Coulomb operator only couples two electrons and can mediate transfer of only one non-separable virtual photon. Of course, the previously discussed SI-ICD pathway remains an allowed pathway under higher-energy conditions with the rate of above, $\Gamma_{SI}^{3e} = 2 \cdot \Gamma^{2e}$, leading eventually to the total three electron rate $\Gamma^{3e} = \Gamma_{SI}^{3e} + \Gamma_{DI}^{3e} = 2 \cdot \Gamma^{2e}$. Conclusively, in both energetic regimes, ICD shall be twice as fast!

Computational Details

For a numerical proof of these hypotheses we perform electron dynamics calculations in one-dimensional QD model potentials with the shape of Gaussians (cf. Fig. 1)

$$V^{1d}(z_i) = \sum_\alpha -D_\alpha \cdot e^{-\frac{4ln(2)}{r_\alpha^2}(z_i - z_\alpha)^2} \tag{7}$$

where the electron index is $i = 1, 2, (3)$ for the two- (three-) electron dynamics and the QD index $\alpha \in [(L), M, R]$. Neighboring QDs are separated by distances $R \in [151.69$ nm; 866.80 nm] for which it was shown that the asymptotic equation is strictly fulfilled.[21] Further, QDs are placed symmetrically on the z axis such that in the two-QD case $z_M = -R/2$ and $z_R = R/2$. In the QD triad case $-z_L = z_R = R$ and $z_M = 0$ nm holds. Note that all variables are given in international system units of GaAs, i.e. we properly account for the effective electron mass approximation in the nanostructure (for details see[13]). The QD shape parameters are leaned to former works for comparability[13] and are $D_M = 10.30$ meV, $D_{L,R} = 8.24$ meV, $2r_M = 36.08$ nm, and $2r_{L,R} = 18.04$ nm for SI-ICD. In the DI case they were altered to $D_M = 15.45$ meV, $D_{L,R} = 6.18$ meV, and $2r_M = 25.51$ nm, with only $2r_{L,R}$ being retained. We desist from accounting for further spatial coordinates, because for vertically-aligned QDs in a wire, strong lateral confinement is assumed. We have shown elsewhere that this one-dimensional approximation gives identical dynamics when we underlie an effective potential approximation for the Coulomb operator as[21,26]

$$V_C^{i,j}(z_i, z_j) = \sqrt{\frac{\pi}{2l^2}}\; e^{\xi^2}\Big(1 - \mathrm{erf}(\xi)\Big). \tag{8}$$

Parameters are $\xi(|z_1 - z_2|) = (\sqrt{\frac{1}{2l^2}}\;|z_1 - z_2|)$ and $l = \sqrt{1/\omega_\perp}$ with a harmonic confinement with frequency $\omega_\perp = 1.0$ a.u. that maps to a lateral QD diameter of $2r_\perp = 28.84$ nm. $\omega_\perp$ was chosen to be equal or larger than typical energy differences in ICD, i.e. E_{vph}, as under these conditions rates are not sensitive to $\omega_\perp$.[27]

We solve the time-dependent Schrödinger equation according to the MCTDH equations of motion[28,29] using the Heidelberg implementation.[30,31] Antisymmetry is now taken into consideration through imposing for all permutations $A_{j_a,j_b,j_c}(t) = -A_{j_b,j_a,j_c}(t)$ and $A_{j_a,j_a,j_c}(t) = 0$ onto the wave function

$$\Psi(z_1, z_2, z_3, t) = \sum_{j_1}\sum_{j_2}\sum_{j_3} A_{j_1,j_2,j_3}(t) \prod_{\kappa=1}^{3} \varphi_{j_\kappa}^{(\kappa)}(z_\kappa, t), \tag{9}$$

which is thus reflecting a quartet state. This spin situation can unequivocally be prepared in charging experiments.[20] The wave function expands onto $j_1 = j_2 = j_3 = 8$ single-particle functions $\varphi_{j_\kappa}^{(\kappa)}(z_\kappa, t)$.

To account for the final continuum state, a basis of 140 sine DVRs (discrete variable representations) within the interval of $[-524$ nm; 524 nm] was used for the identical electrons. An nth-order complex absorbing potential near the grids' ends (± 325 nm) removes the wave packet of the scattered ICD electron from the system.[13]

Results

Single-Ionization Energy Regime

The SI-ICD system incorporates single-electron level energies $E_{M0} = -7.15$ meV and $E_{M1} = -2.01$ meV for the photon-emitting QD and $E_{L0} = E_{R0} = -3.61$ meV for the electron-emitting QDs. This gives rise to the energy condition known from former works, namely the state ordering $E_{M1} > E_{L0} = E_{R0} > E_{M0}$. The virtual photon energy $E_{vph} \approx E_{M1} - E_{M0} = 5.14$ meV exceeds once, but not twice the ionization potential $IP = 3.61$ meV of the electron-emitting LQD and RQD.

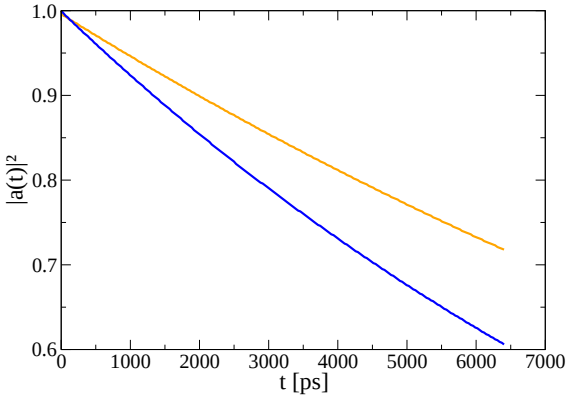

Figure 2: (Color online) The absolute squared autocorrelation function $|a(t)|^2$ as function of time decays exponentially as shown here for $R = 195.03$ nm. For the n-electron n-QD ICD with $n = 2$ an orange/gray line is used, for $n = 3$ a blue/black line.

In comparing the dynamics we first focus on the example of $R = 195$ nm for which

the exponential decay of the squared autocorrelation function $|a(t)|^2 = |\langle d|\Psi(t)\rangle|^2 = e^{-\Gamma t}$ confirms ICD not only for the QD pair case (orange/gray line in Fig. 2), but most importantly for the tree-electron case (blue/black line). Further, the projections of the wave function onto the single-electron state functions ϕ^n, which we do not show here, reveal that the electron in the MQD relaxes on the same time scale. Further, one of the indistinguishable electrons in the small QDs is excited into the electronic continuum, but in fact due to the superposition of the two ionization channels $L_0 \to C$ and $R_0 \to C$ one cannot assign which electron this is and one will observe ionization from both QDs to the same amount. The two-electron two-QD rates obtained for $R = 195$ nm are $\Gamma^{2e} = 3.4 \cdot 10^{-5}$ meV in agreement with findings from former studies[13] and $\Gamma^{3e} = 5.1 \cdot 10^{-5}$ meV, which is indeed larger. However, the ratio of rates $\Gamma^{3e}/\Gamma^{2e} = 1.5 \neq 2.0$ cannot confirm the hypothesis (Eq. (5))!

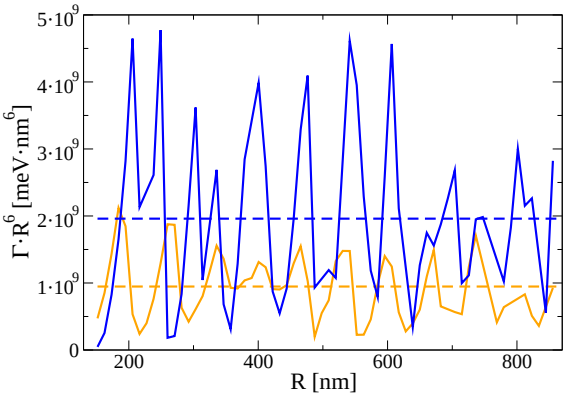

Figure 3: (Color online) The ICD rates Γ multiplied with R^6 for two (orange/gray) and three electrons (blue/black) are displayed for 151.69 nm $\leq R \leq$ 866.80 nm. The average values $\overline{\Gamma^{2e}R^6}$ and $\overline{\Gamma^{3e}R^6}$ for each series of rates are inserted as dashed lines.

Widening our view onto former studies on quasi or truly one-dimensional paired QDs, we are aware of oscillations of the rate Γ^{2e} around R^{-6}.[13,32] They originate, at least to a certain extend, from the Coulomb barrier which the ICD electron senses when nearing the remaining electron in the MQD which it can either tunnel (enhanced Γ^{2e}) or not (reduced Γ^{2e}). The same type of oscillations are found for Γ^{3e} as function of R. With two neighboring electrons the oscillations are, however, not synchronous with the ones in the two-electron case which ultimately leads to ratios $\Gamma^{3e}/\Gamma^{2e}(R)$ spanning over $[0.1; 17.5]$ for all sampled R.

Therefore, for a meaningful analysis of the asymptotic behavior we plot $\Gamma \cdot R^6$ in Fig. 3 with the color code of before. This quantity is constant besides the Coulomb barrier-induced oscillations. Both averages $\overline{\Gamma \cdot R^6}$ are inserted as dashed lines. And indeed, here we obtain $\overline{\Gamma^{3e} R^6}/\overline{\Gamma^{2e} R^6} = 2.07$ with a standard deviation of 1.68, finally confirming $\Gamma^{3e} = 2 \cdot \Gamma^{2e}$ for the SI-ICD process.

Double-Ionization Energy Regime

The very same analyses are performed for the DI case. The system has MQD energies $E_{M0} = -10.11$ meV, $E_{M1} = -1.89$ meV, i.e. the virtual photon energy is higher with $E_{vph} \approx E_{M1} - E_{M0} = 8.22$ meV. The energies of the adjacent QDs' levels are $E_{L0} = E_{R0} = -2.39$ meV so that twice the IP is lower than E_{vph} and the DI channel is open. The calculations turned out to be less stable than the previous ones, making it impossible to analyze particularly Γ^{3e} beyond $R = 249.09$ nm. But even in this smaller R interval the ratio of the averages is obtained as $\overline{\Gamma^{3e} R^6}/\overline{\Gamma^{2e} R^6} = 1.88$ with a standard deviation of 0.67. So also in this case $\Gamma^{3e} = 2 \cdot \Gamma^{2e}$ is confirmed in accord with the rationalizations.

Let us mention at this place one other recent study considering DI-ICD.[19] The targeted system was an alkali dimer adjacent to a He droplet in which one excited He atom relaxes by ionizing both alkali atoms. This was detected in coincidence measurements, where the triple coincidence of one electron and both alkali cations gives a DI-ICD trace with lower kinetic energies of the electron than the double coincidence of the electron and just one cation, mapping both DI-ICD and SI-ICD. This is contradictory to the suppression of DI-ICD that we find here. Explanations may be that in the He droplet system the asymptotic equation (Eq. (6)) is not valid. Possible reasons could be the large number of non-participating electrons that nonetheless correlate to the active ones or the differing geometry with angles less than 180° among neighbors and distance small enough to not forbid electron transfer. Future investigations on the differences of both systems are necessary to clarify this discrepancy.

Discussion

With having established here three-electron dynamics MCTDH calculations in QDs, the wealth of other three- and more-electron processes in assemblies of QDs is within reach and will allow for further predictions, e.g. of superexchange ICD[33,34] or the inverse process to this one here,[35–37] for all relevant energetic cases. One other systematic improvement of the methodology has been recently achieved, which is the description of a two-dimensional continuum in the electron dynamics[32] reflecting thus self-assembled[38,39] and lithographic QD.[40] Such extended continuum winds down the oscillatory behavior of continuum electrons with distance,[32] which will allow for a clearer analysis of three-electron three-QD ICD. In such systems electron dynamics investigations can enhance significantly the insight into the dependence of ICD on the relative positions of QDs.

For an experimental proof of ICD in the above described model system one needs to grow a quantum wire in which the three QDs are either of a lower band-gap material than the wire material[20,41] or, preferably, realized through placing electrostatic gates for electron confinement along the wire.[40] For different QD distances, different wires are to be grown or different gates to be placed. Further, the setup requires a gate circuit along the wire for singly-charging each QD with same-spin electrons.[20,41,42] To induce ICD an infrared source is needed that is focused through a shadowmask[43] in order to selectively excite the MQD. For optimal performance we suggest it to have the energy of the virtual photon, an intensity of 1.37 $\mathrm{kWcm^{-2}}$ and a pulse duration of 14.1 ps.[44] For analysis there are as well several options. Either one detects the current induced by the ICD electrons through the wire,[20,40] which reflects the absorbance of an electron by a complex absorbing potential in the calculation and could allow for a comparison of electron spectra.[13,45] Otherwise pump-probe[46] or photocurrent techniques[47] as well as electrodes as charge sensors[20,40] at each QD can be used to determine the electron occupation numbers in the QDs which correspond to the calculated projections.

Regarding the QD placement in the wire we strongly recommend to stick to the shortest

of the investigated distances, i.e. 150 - 200 nm, where rates are in the order of about 10^{-5} meV (10^4 ps), because here ICD may dominate phonon-mediated decay and emission[14] or radiative decay[13] happening both on a nanosecond time scale. Even lower distances (80 nm) not investigated here are recommendable, where ICD is as fast as 150 ps,[13] with the drawback that the asymptotic equation does not strictly apply. At even shorter distances that allow for electron transfer among the QDs, ICD may not be exclusive but overlaid by the electron-transfer mediated decay process[48] leading to the same final state. Circumventing these drawback of GaAs QDs, rate enhancement by three-electron ICD can as an alternative be proven in QDs of other materials, e.g. AlN,[13] in triads of overall smaller measures,[13] as well as in atomic or molecular trimers in which ICD is in general orders of magnitude faster and less likely subject to competing decay processes. As our model and results are universal to various electron binding systems, such consideration is well allowed.

Conclusions

The overall conclusion of this study is that when a QD pair capable of ICD is extended into a triad by another electron-emitting QD in the row next to the excited one, then the ICD rate doubles. We come to this conclusion by a detailed rationalization of the energetics based on the Wigner-Weisskopf rate and confirm it by numerical electron dynamics calculations that go beyond previous non-Hermitian electronic structure calculations for the example of neon clusters because they allow for time-resolution and tailor-made energy conditions. Absolute rates are obtained for GaAs QDs of a certain geometry, but due to the generality of the approach the result on rate doubling is universal for other QD materials or geometries as well as atoms and molecules that are capable of ICD under fulfillment of the energy and distance conditions which allow a virtual-photon description.

Acknowledgement

We gratefully acknowledge financial and idealistic support from the Volkswagen Foundation through the Freigeist Fellowship No. 89525. Further we like to thank our first reviewer for their comments that helped to make the Theory section accurate.

References

(1) Lerner, E.; Cordes, T.; Ingargiola, A.; Alhadid, Y.; Chung, S.; Michalet, X.; Weiss, S. Toward Dynamic Structural Biology: Two Decades of Single-Molecule Förster Resonance Energy Transfer. *Science* **2018**, *359*, eaan1133.

(2) Kamat, P. V. Meeting the Clean Energy Demand: Nanostructure Architectures for Solar Energy Conversion. *J. Phys. Chem. C* **2007**, *111*, 2834–2860.

(3) Cederbaum, L. S.; Zobeley, J.; Tarantelli, F. Giant Intermolecular Decay and Fragmentation of Clusters. *Phys. Rev. Lett.* **1997**, *79*, 4778–4781.

(4) Jahnke, T. Interatomic and Intermolecular Coulombic Decay: The Coming of Age Story. *J. Phys. B: At. Mol. Opt. Phys.* **2015**, *48*, 082001.

(5) Ren, X.; Wang, E.; Skitnevskaya, A. D.; Trofimov, A. B.; Gokhberg, K.; Dorn, A. Experimental Evidence for Ultrafast Intermolecular Relaxation Processes in Hydrated Biomolecules. *Nat. Phys.* **2018**, *14*, 1062–1066.

(6) Xu, S.; Guo, D.; Ma, X.; Zhu, X.; Feng, W.; Yan, S.; Zhao, D.; Gao, Y.; Zhang, S.; Ren, X. et al. Damaging Intermolecular Energy and Proton Transfer Processes in Alpha-Particle-Irradiated Hydrogen-Bonded Systems. *Angew. Chem. Int. Ed.* **2018**, *57*, 17023–17027.

(7) Wilhelm, R. A.; Gruber, E.; Schwestka, J.; Kozubek, R.; Madeira, T. I.; Marques, J. P.; Kobus, J.; Krasheninnikov, A. V.; Schleberger, M.; Aumayr, F. Interatomic Coulombic

Decay: The Mechanism for Rapid Deexcitation of Hollow Atoms. *Phys. Rev. Lett.* **2017**, *119*, 103401.

(8) Cederbaum, L. S. Ultrafast Intermolecular Energy Transfer from Vibrations to Electronic Motion. *Phys. Rev. Lett.* **2018**, *121*, 223001.

(9) Averbukh, V.; Cederbaum, L. S. Interatomic Electronic Decay in Endohedral Fullerenes. *Phys. Rev. Lett.* **2006**, *96*, 053401.

(10) De, R.; Magrakvelidze, M.; Madjet, M. E.; Manson, S. T.; Chakraborty, H. S. First Prediction of Inter-Coulombic Decay of C60 Inner Vacancies Through the Continuum of Confined Atoms. *J. Phys. B: At. Mol. Opt. Phys.* **2016**, *49*, 11LT01.

(11) Goldzak, T.; Gantz, L.; Gilary, I.; Bahir, G.; Moiseyev, N. Vertical Currents due to Interatomic Coulombic Decay in Experiments with Two Coupled Quantum Wells. *Phys. Rev. B* **2016**, *93*, 045310.

(12) Cherkes, I.; Moiseyev, N. Electron Relaxation in Quantum Dots by the Interatomic Coulombic Decay Mechanism. *Phys. Rev. B* **2011**, *83*, 113303.

(13) Bande, A.; Gokhberg, K.; Cederbaum, L. S. Dynamics of Interatomic Coulombic Decay in Quantum Dots. *J. Chem. Phys.* **2011**, *135*, 144112.

(14) Bande, A. Acoustic Phonon Impact on the Inter-Coulombic Decay Process in Charged Quantum Dot Pairs. *Mol. Phys.* **2019**, *117*, 2014–2028

(15) Santra, R.; Cederbaum, L. S. Non-Hermitian Electronic Theory and Applications to Clusters. *Phys. Rep.* **2002**, *368*, 1–117.

(16) Santra, R.; Zobeley, J.; Cederbaum, L. S. Electronic Decay of Valence Holes in Clusters and Condensed Matter. *Phys. Rev. B* **2001**, *64*, 245104.

(17) Reimann, S. M.; Manninen, M. Electronic Structure of Quantum Dots. *Rev. Mod. Phys.* **2002**, *74*, 1283–1342.

(18) Bera, D.; Qian, L.; Tseng, T.-K.; Holloway, P. H. Quantum Dots and Their Multimodal Applications: A Review. *Materials* **2010**, *3*, 2260–2345.

(19) LaForge, A. C.; Shcherbinin, M.; Stienkemeier, F.; Richter, R.; Moshammer, R.; Pfeifer, T.; Mudrich, M. Highly Efficient Double Ionization of Mixed Alkali Dimers by Intermolecular Coulombic Decay. *Nat. Phys.* **2019**, *15*, 247–250.

(20) Salfi, J.; Roddaro, S.; Ercolani, D.; Sorba, L.; Savelyev, I.; Blumin, M.; Ruda, H. E.; Beltram, F. Electronic Properties of Quantum Dot Systems Realized in Semiconductor Nanowires. *Semicond. Sci. Technol.* **2010**, *25*, 024007.

(21) Bande, A.; Pont, F. M.; Dolbundalchok, P.; Gokhberg, K.; Cederbaum, L. S. Dynamics of Interatomic Coulombic Decay in Quantum Dots: Singlet Initial State. *EPJ Web Conf.* **2013**, *41*, 04031.

(22) Averbukh, V.; Müller, I. B.; Cederbaum, L. S. Mechanism of Interatomic Coulombic Decay in Clusters. *Phys. Rev. Lett.* **2004**, *93*, 263002.

(23) Averbukh, V.; Cederbaum, L. S. Ab initio calculation of interatomic decay rates by a combination of the Fano ansatz, Green's-function methods, and the Stieltjes imaging technique. *J. Chem. Phys.* **2005**, *123*, 204107.

(24) Katsuura, K. Ionization of Atoms by Collision with Excited Atoms. *J. Chem. Phys.* **1965**, *42*, 3771–3775.

(25) Matthew, J. A. D.; Komninos, Y. Transition rates for interatomic Auger processes. *Surf. Sci.* **1975**, *53*, 716–725.

(26) Bednarek, S.; Szafran, B.; Chwiej, T.; Adamowski, J. Effective Interaction for Charge Carriers Confined in Quasi-One-Dimensional Nanostructures. *Phys. Rev. B* **2003**, *68*, 045328.

(27) Dolbundalchok, P.; Peláez, D.; Aziz, E.; Bande, A. Geometrical Control of the Interatomic Coulombic Decay Process in Quantum Dots. *J. Comput. Chem.* **2016**, *37*, 2249 – 2259.

(28) Meyer, H.-D.; Manthe, U.; Cederbaum, L. S. The Multi-Configurational Time-Dependent Hartree Approach. *Chem. Phys. Lett.* **1990**, *165*, 73–78.

(29) Manthe, U.; Meyer, H.-D.; Cederbaum, L. S. Wave-Packet Dynamics within the Multiconfiguration Hartree Framework: General Aspects and Application to NOCl. *J. Chem. Phys.* **1992**, *97*, 3199–3213.

(30) Beck, M. H.; Jäckle, A.; Worth, G. A.; Meyer, H.-D. The Multiconfiguration Time-Dependent Hartree (MCTDH) Method: a Highly Efficient Algorithm for Propagating Wavepackets. *Phys. Rep.* **2000**, *324*, 1–105.

(31) Meyer, H.-D., Gatti, F., Worth, G. A., Eds. *Multidimensional Quantum Dynamics*; Wiley-VCH, 2009.

(32) Haller, A.; Peláez, D.; Bande, A. Prediction of the Interatomic Coulombic Decay Process in Laterally Arranged Pairs of Self-Assembled Quantum Dots. *J. Phys. Chem. C* **2019**, *123*, 14754–14765

(33) Miteva, T.; Kazandjian, S.; Kolorenč, P.; Votavová, P.; Sisourat, N. Interatomic Coulombic Decay Mediated by Ultrafast Superexchange Energy Transfer. *Phys. Rev. Lett.* **2017**, *119*, 083403.

(34) Bennett, R.; Votavová, P.; Kolorenč, P.; Miteva, T.; Sisourat, N.; Buhmann, S. Y. Virtual Photon Approximation for Three-Body Interatomic Coulombic Decay . *Phys. Rev. Lett.* **2019**, *122*, 153401.

(35) Averbukh, V.; Kolorenč, P. Collective Interatomic Decay of Multiple Vacancies in Clusters. *Phys. Rev. Lett.* **2009**, *103*, 183001.

(36) Kuleff, A. I.; Gokhberg, K.; Kopelke, S.; Cederbaum, L. S. Ultrafast Interatomic Electronic Decay in Multiply Excited Clusters. *Phys. Rev. Lett.* **2010**, *105*, 043004.

(37) Müller, C.; Macovei, M. A.; Voitkiv, A. B. Collectively Enhanced Resonant Photoionization in a Multiatom Ensemble. *Phys. Rev. A* **2011**, *84*, 055401.

(38) Wang, L.; Rastelli, A.; Kiravittaya, S.; Benyoucef, M.; Schmidt, O. G. Self-Assembled Quantum Dot Molecules. *Adv. Mater.* **2009**, *21*, 2601–2618.

(39) Zallo, E.; Atkinson, P.; Wang, L.; Rastelli, A.; Schmidt, O. G. Epitaxial Growth of Lateral Quantum Dot Molecules. *Phys. Status Solidi B* **2012**, *249*, 702–709.

(40) van der Wiel, W. G.; De Franceschi, S.; Elzerman, J. M.; Fujisawa, T.; Tarucha, S.; Kouwenhoven, L. P. Electron Transport Through Double Quantum Dots. *Rev. Mod. Phys.* **2002**, *75*, 1–22.

(41) Roddaro, S.; Pescaglini, A.; Ercolani, D.; Sorba, L.; Beltram, F. Manipulation of Electron Orbitals in Hard-Wall InAs/InP Nanowire Quantum Dots. *Nano Lett.* **2011**, *11*, 1695–1699.

(42) Nadj-Perge, S.; Pribiag, V. S.; van den Berg, J. W. G.; Zuo, K.; Plissard, S. R.; Bakkers, E. P. A. M.; Frolov, S. M.; Kouwenhoven, L. P. Spectroscopy of Spin-Orbit Quantum Bits in Indium Antimonide Nanowires. *Phys. Rev. Lett.* **2012**, *108*, 166801.

(43) Luo, J.; Lai, W.; Lu, D.; Du, C.; Liu, Y.; Gong, S.; Shi, D.; Guo, C. Pronounced Enhancement of Exciton Rabi Oscillation for a Two-Photon Transition Based on Quantum Dot Coupling Control. *J. Phys. B: At. Mol. Opt. Phys.* **2012**, *45*, 035402.

(44) Haller, A.; Bande, A. Favoritism of Quantum Dot Inter-Coulombic Decay over Direct and Multi-Photon Ionization by Laser Strength and Focus. *J. Chem. Phys.* **2018**, *149*, 134102.

(45) Bande, A. Dynamics of Interatomic Coulombic Decay in Quantum Dots Induced by a Laser Field. *J. Chem. Phys.* **2013**, *138*, 214104.

(46) Müller, K.; Bechtold, A.; Ruppert, C.; Zecherle, M.; Reithmaier, G.; Bichler, M.; Krenner, H. J.; Abstreiter, G.; Holleitner, A. W.; Villas-Boas, J. M.; Betz, M.; Finley, J. J. Electrical Control of Interdot Electron Tunneling in a Double InGaAs Quantum-Dot Nanostructure. *Phys. Rev. Lett.* **2012**, *108*, 197402.

(47) Fry, P. W.; Finley, J. J.; Wilson, L. R.; Lemaître, A.; Mowbray, D. J.; Skolnik, S.; Hopkinson, M.; Hill, G.; Clark, J. C. Electric-Field-Dependent Carrier Capture and Escape in Self-Assembled InAs/GaAs Quantum Dots. *Appl. Phys. Lett.* **2000**, *77*, 4344–4346.

(48) Zobeley, J.; Santra, R.; Cederbaum, L. S. Electronic decay in weakly bound heteroclusters: Energy transfer versus electron transfer. *J. Chem. Phys.* **2001**, *115*, 5076–5088.

Graphical TOC Entry